Outage-Aware Secure Beamforming in MISO Wireless Interference Networks

Zhichao Sheng, Hoang Duong Tuan, Trung Q. Duong, and H. Vincent Poor

Abstract—**Based on the knowledge of the channel distributions of a multi-input single-output wireless network of multiple transmitter-user pairs overheard by an eavesdropper, this letter develops an outage-aware beamforming design to optimize the users' quality-of-service (QoS) in terms of their secrecy rates. This is a very computationally difficult problem with a nonconcave objective function and nonlinear equality constraints in beamforming vectors. A path-following algorithm of low-complexity and rapid convergence is proposed for computation, which is also extended to solving the problem of maximizing the network's secure energy efficiency under users' QoS constraints. Numerical examples are provided to verify the efficiency of the proposed algorithms.**

Index Terms—**Energy-efficient communication, interference networks, outage-aware beamforming, path-following algorithms, secure communication.**

I. Introduction

SECURE beamforming to maximize the so-called secrecy rate, which is the difference of the user rate and rate at an eavesdropper (EV), has proved to be useful in wireless physical layer security (see, e.g., [1]–[4] and references therein). The most popular secure beamforming design is based on the current channel state obtained from channel estimation [1], [3]–[6]. This design is more practical for slow fading channels, which do not need frequent channel estimation. On the other hand, the channel distribution information (CDI) does not need to be updated for a relatively long period of time because the channel distribution usually evolves very slowly. Therefore, CDI-based secure beamforming to maximize the secrecy rate under transmission outage probability constraints is of practical interest but has not yet been appropriately addressed in the literature. CDI-based conventional beamforming design, which aims to maximize the user rate only, already leads to very complicated nonlinear optimization problems involving nonlinear equality constraints [7], [8].

Manuscript received March 14, 2018; revised April 19, 2018; accepted April 19, 2018. Date of publication May 2, 2018; date of current version May 23, 2018. This work was supported in part by the U.S. National Science Foundation under Grants CNS-1702808 and ECCS-1647198. The associate editor coordinating the review of this manuscript and approving it for publication was Prof. Yong Xiang. *(Corresponding author: Hoang Duong Tuan.)*

Z. Sheng and H. D. Tuan are with the School of Electrical and Data Engineering, University of Technology Sydney, Broadway, NSW 2007, Australia (e-mail: zhichaosheng@163.com; Tuan.Hoang@uts.edu.au).

T. Q. Duong is with the Queen's University Belfast, Belfast BT7 1NN, U.K. (e-mail: trung.q.duong@qub.ac.uk).

H. V. Poor is with the Department of Electrical Engineering, Princeton University, Princeton, NJ 08544 USA (e-mail: poor@princeton.edu).

Color versions of one or more of the figures in this letter are available online at http://ieeexplore.ieee.org.

Digital Object Identifier 10.1109/LSP.2018.2829663

This letter aims to address the problem of CDI-based secure beamforming for a network of multiple transmitter–user pairs with the presence of an EV. Our contribution is to propose a path-following computational procedure of low complexity for its solution. Furthermore, such a path-following computational procedure is extended to maximize the secure energy efficiency (SEE), which is the ratio of the secrecy rate to the total network power consumption, measured in terms of secrecy bits per Joule per Hertz [6], [9]. Unlike the existing results [4], [10], we show that this SEE problem is not more computationally difficult than the above aforementioned secured beamforming problem.

The paper is organized as follows. After this introduction, Section II is devoted to the problem formulations. Algorithms for secrecy rate maximization and energy efficiency maximization are developed in Sections III and IV, respectively. Simulations to demonstrate the efficiencies of these algorithms are provided in Section V. Section VI concludes the paper.

Notation: Optimization variables are boldfaced. The notation $\sum_{j\neq i}^{M}$ refers to the summation taken over the index set $\mathcal{M}\setminus\{i\}$ for $\mathcal{M}\triangleq\{1,\ldots,M\}$. $\mathcal{CN}(0,I)$ is the set of complex Gaussian variables of zero mean and identity covariance, while $C(0,1)$ is the set of real scalar Gaussian variables of zero mean and unit covariance.

II. Problem Statements

Consider a communication network of M transmitter–user pairs overheard by an EV. Each transmitter is equipped with N_t transmit antennas, while each of the users and the EV is equipped with a single antenna. Thus, in the absence of the EV, the network looks very much like that considered in [7], [8], [11], and [12]. The information signal s_i for user i, which is normalized as $E(s_i^2)=1$, is beamformed by $\mathbf{w}_i\in\mathbb{C}^{N_t}$. The received signal at user i is

$$y_i = h_{ii}^H\mathbf{w}_i s_i + \sum_{j\neq i}^{M} h_{ji}^H\mathbf{w}_j s_j + n_i, i\in\mathcal{M}$$

where $h_{ji}\in\mathbb{C}^{N_t}$ is the vector channel from transmitter j to user i and $n_i\in\mathcal{CN}(0,\sigma_i^2)$ is the background noise. Analogously, the received signal at the EV is

$$y_E = \sum_{i=1}^{M} h_{ie}^H\mathbf{w}_i s_i + n_e$$

where $h_{ie}\in\mathbb{C}^{N_t}$ is the vector channel from transmitter i to the EV and $n_e\in\mathcal{CN}(0,\sigma_e^2)$ is the background noise.

In the paper, we assume that $h_{ji}=\sqrt{\bar{h}_{ji}}\chi_{ji}$, $\chi_{ji}\in\mathcal{CN}(0,I)$ and $h_{je}=\sqrt{\bar{h}_{je}}\chi_j$, $\chi_j\in\mathcal{CN}(0,I)$, where $\bar{h}_{ji}$ and $\bar{h}_{je}$ are known deterministic quantities indicating the strength of the corresponding channels.

Let $\mathbf{w} \triangleq [\mathbf{w}_i]_{i\in\mathcal{M}} \in \mathbb{C}^{MN_t}$. Introduce scalar variables $\mathbf{R}_i > 0$ and $\mathbf{r}_i > 0$ and define the functions

$$f_{i,o}(\mathbf{R}_i, \mathbf{w}) \triangleq \bar{h}_{ii} \ln(1-\epsilon) + \sigma_i^2 \frac{\mathbf{R}_i}{||\mathbf{w}_i||^2} + \bar{h}_{ii} \sum_{j\neq i}^M \ln\left(1 + \frac{\mathbf{R}_i \bar{h}_{ji} ||\mathbf{w}_j||^2}{\bar{h}_{ii}||\mathbf{w}_i||^2}\right)$$

for $\epsilon > 0$ and

$$g_{i,o}(\mathbf{r}_i, \mathbf{w}) \triangleq \bar{h}_{ie} \ln(1-\epsilon_{\rm EV}) + \sigma_e^2 \frac{\mathbf{r}_i}{||\mathbf{w}_i||^2} + \bar{h}_{ie} \sum_{j\neq i}^M \ln\left(1 + \frac{\mathbf{r}_i \bar{h}_{je} ||\mathbf{w}_j||^2}{\bar{h}_{ie}||\mathbf{w}_i||^2}\right)$$

for $\epsilon_{\rm EV} > 0$. User i's rate in nats is defined through the outage probability as $\max\left\{ \ln(1+\mathbf{R}_i) : \text{Prob}\left(\frac{\bar{h}_{ii}|\chi_{ii}^H \mathbf{w}_i|^2}{\sum_{j\neq i}^M \bar{h}_{ji}|\chi_{ji}^H \mathbf{w}_j|^2 + \sigma_i^2} < \mathbf{R}_i\right) < \epsilon\right\}$, which by [13] is $\ln(1+\mathbf{R}_i)$ with $\mathbf{R}_i$ satisfying the nonlinear equation

$$f_{i,o}(\mathbf{R}_i, \mathbf{w}) = 0. \tag{1}$$

Analogously, the rate in nats for user i at the EV is defined by $\max\left\{ \ln(1+\mathbf{r}_i) : \text{Prob}\left(\frac{\bar{h}_{ie}|\chi_i^H \mathbf{w}_i|^2}{\sum_{j\neq i}^M \bar{h}_{je}|\chi_j^H \mathbf{w}_j|^2 + \sigma_e^2} < \mathbf{r}_i\right) < \epsilon_{\rm EV}\right\}$, which is $\ln(1+\mathbf{r}_i)$ with $\mathbf{r}_i$ satisfying the nonlinear equation

$$g_{i,o}(\mathbf{r}_i, \mathbf{w}) = 0. \tag{2}$$

User i's secrecy rate is defined as $\varphi_i(\mathbf{R}_i, \mathbf{r}_i) \triangleq \ln(1+\mathbf{R}_i) - \ln(1+\mathbf{r}_i)$. We will address the following optimization problems in $\mathbf{w}$, $\mathbf{R} \triangleq [\mathbf{R}_i]_{i\in\mathcal{M}}$ and $\mathbf{r} \triangleq [\mathbf{r}_i]_{i\in\mathcal{M}}$.

1) Secrecy rate maximin optimization under transmitter power constraints:

$$\max_{\boldsymbol{w},\mathbf{R},\mathbf{r}} \Phi(\mathbf{R}, \mathbf{r}) \triangleq \min_{i\in\mathcal{M}} \varphi_i(\mathbf{R}_i, \mathbf{r}_i) \quad \text{s.t.} \quad (1), (2) \tag{3a}$$

$$||\mathbf{w}_i||^2 \le P_i, i \in \mathcal{M} \tag{3b}$$

with P_i chosen to set the limit of transmission power at transmitter i.

2) Energy efficiency maximization over the secrecy rate threshold constraints:

$$\max_{\boldsymbol{w},\mathbf{R},\mathbf{r}} \Theta(\mathbf{w}, \mathbf{R}, \mathbf{r}) \triangleq \frac{\sum_{i=1}^M \varphi_i(\mathbf{R}_i, \mathbf{r}_i)}{\pi(\mathbf{w})} \quad \text{s.t.} \quad (1), (2), (3b), \tag{4a}$$

$$\varphi_i(\mathbf{R}_i, \mathbf{r}_i) \ge c_i, \ i \in \mathcal{M} \tag{4b}$$

with c_i chosen to set the quality-of-service (QoS) threshold for user i and the total network power consumption $\pi(\mathbf{w}) \triangleq \zeta \sum_{i\in\mathcal{M}} ||\mathbf{w}_i||^2 + P_c$ in transmitting $\mathbf{w}_i s_i$, where $0 < \zeta < 1$ is the reciprocal of the drain efficiency of the power amplifier and $P_c = \sum_{i\in\mathcal{M}} P_c^i$ with circuit power P_c^i at transmitter i.

III. Secrecy Rate Maximization

The nonlinear equality constraints (1) and (2) not only cause tough computational challenges, but also make the interior of the feasibility set of problem (3) empty. As such, a path-following algorithm, which involves an inner approximation for its feasibility set, is impossible. Similar to [13],[1] by using the fact that $f_{i,o}(\mathbf{R}_i, \mathbf{w})$ and $g_{i,o}(\mathbf{r}_i, \mathbf{w})$ are increasing functions in $\mathbf{R}_i$ and $\mathbf{r}_i$, we can show that (3) is equivalent to

$$\max_{\boldsymbol{w},\mathbf{R},\mathbf{r}} \Phi(\mathbf{R}, \mathbf{r}) \quad \text{s.t.} \quad (3b), \tag{5a}$$

$$\mathbf{R}_i > 0, \mathbf{r}_i > 0, i \in \mathcal{M}, \tag{5b}$$

$$f_{i,o}(\mathbf{R}_i, \mathbf{w}) \le 0, i \in \mathcal{M}, \tag{5c}$$

$$g_{i,o}(\mathbf{r}_i, \mathbf{w}) \ge 0, \ i \in \mathcal{M} \tag{5d}$$

where the nonlinear equality constraints (1) and (2) are replaced by their one-sided inequality constraints (5c) and (5d), which are nonconvex constraints. To develop a path-following algorithm for solving (5), which generates a sequence of improved feasible points, we need to provide a lower bounding approximation for the objective function in (5a) as well as inner approximations for constraints (5c) and (5d).

Suppose $(w^{(\kappa)}, R^{(\kappa)}, r^{(\kappa)})$ is a feasible point for (5) found from the $(\kappa-1)$th iteration. Following [13], the secrecy rate function $\varphi_i(\mathbf{R}_i, \mathbf{r}_i)$ is lower bounded as $\varphi_i(\mathbf{R}_i, \mathbf{r}_i) \ge \varphi_i^{(\kappa)}(\mathbf{R}_i, \mathbf{r}_i) \triangleq A_i^{(\kappa)}(\mathbf{R}_i) - a_i^{(\kappa)}(\mathbf{r}_i)$, where $A_i^{(\kappa)}(\mathbf{R}_i) \triangleq \ln(1+R_i^{(\kappa)}) + \frac{R_i^{(\kappa)}}{R_i^{(\kappa)}+1} - \frac{(R_i^{(\kappa)})^2}{R_i^{(\kappa)}+1}\frac{1}{\mathbf{R}_i}$, which is a concave function, and $a_i^{(\kappa)}(\mathbf{r}_i) \triangleq \ln(1+r_i^{(\kappa)}) - \frac{r_i^{(\kappa)}}{r_i^{(\kappa)}+1} + \frac{\mathbf{r}_i}{r_i^{(\kappa)}+1}$, which is a linear function. Therefore, the objective $\Phi(\mathbf{R}, \mathbf{r})$ in (5a) is bounded by

$$\Phi(\mathbf{R}, \mathbf{r}) \ge \Phi^{(\kappa)}(\mathbf{R}, \mathbf{r}) \triangleq \min_{i=1,\dots,M} \varphi_i^{(\kappa)}(\mathbf{R}_i, \mathbf{r}_i). \tag{6}$$

For $\alpha_{ij}^{(\kappa)} \triangleq R_i^{(\kappa)} \bar{h}_{ji} ||w_j^{(\kappa)}||^2 / \bar{h}_{ii} ||w_i^{(\kappa)}||^2 > 0$, and $\beta_{ij}^{(\kappa)} \triangleq \bar{h}_{ii}\left(\ln(1+\alpha_{ij}^{(\kappa)}) - \alpha_{ij}^{(\kappa)}/(1+\alpha_{ij}^{(\kappa)})\right) > 0$, one has

$$\begin{aligned}
&\bar{h}_{ii}||\mathbf{w}_i||^2 \ln\left(1 + \frac{\mathbf{R}_i \bar{h}_{ji}||\mathbf{w}_j||^2}{\bar{h}_{ii}||\mathbf{w}_i||^2}\right) \\
&\le \bar{h}_{ii}||\mathbf{w}_i||^2 \left(\ln(1+\alpha_{ij}^{(\kappa)}) - \frac{\alpha_{ij}^{(\kappa)}}{1+\alpha_{ij}^{(\kappa)}} \right. \\
&\left. + \frac{\mathbf{R}_i \bar{h}_{ji}||\mathbf{w}_j||^2}{(1+\alpha_{ij}^{(\kappa)})\bar{h}_{ii}||\mathbf{w}_i||^2}\right) = \beta_{ij}^{(\kappa)}||\mathbf{w}_i||^2 + \frac{\bar{h}_{ji}}{1+\alpha_{ij}^{(\kappa)}} \mathbf{R}_i ||\mathbf{w}_j||^2 \\
&\le \beta_{ij}^{(\kappa)}||\mathbf{w}_i||^2 + \frac{\bar{h}_{ji}}{1+\alpha_{ij}^{(\kappa)}} \left(\frac{||w_j^{(\kappa)}||^2}{2R_i^{(\kappa)}} \mathbf{R}_i^2 + \frac{R_i^{(\kappa)}}{2||w_j^{(\kappa)}||^2}||\mathbf{w}_j||^4\right).
\end{aligned}$$

For the convex function $\gamma_i^{(\kappa)}(\mathbf{R}_i, \mathbf{w}) \triangleq \sum_{j\neq i}^M \left(\beta_{ij}^{(\kappa)}||\mathbf{w}_i||^2 + \frac{\bar{h}_{ji}}{2(1+\alpha_{ij}^{(\kappa)})}\left(\frac{||w_j^{(\kappa)}||^2}{R_i^{(\kappa)}}\mathbf{R}_i^2 + \frac{R_i^{(\kappa)}}{||w_j^{(\kappa)}||^2}||\mathbf{w}_j||^4\right)\right)$, the nonconvex constraint (5c) is innerly approximated by the following convex constraint:

$$\left(2\Re\{(w_i^{(\kappa)})^H \mathbf{w}_i\} - ||w_i^{(\kappa)}||^2\right) \bar{h}_{ii} \ln(1-\epsilon) + \sigma_i^2 \mathbf{R}_i + \gamma_i^{(\kappa)}(\mathbf{R}_i, \mathbf{w}) \le 0, i \in \mathcal{M}. \tag{7}$$

[1] Sheng *et al.* [13] considered power allocation for single-input single-output networks, which is much simpler than beamforming for MISO networks considered in the present paper. Moreover, the channel paths in [13] are assumed to be deterministic with probabilistic error.

Applying inequality (69) from [14] for $x = 1/\mathbf{r}_i \bar{h}_{je}||\mathbf{w}_j||^2$, $y = \bar{h}_{ie}||\mathbf{w}_i||^2$, and $\bar{x} = 1/r_i^{(\kappa)}\bar{h}_{je}||w_j^{(\kappa)}||^2$, $\bar{y} = \bar{h}_{ie}||w_i^{(\kappa)}||^2$ yields

$$\ln\left(1 + \frac{\mathbf{r}_i \bar{h}_{je}||\mathbf{w}_j||^2}{\bar{h}_{ie}||\mathbf{w}_i||^2}\right) \geq \lambda_{ij}^{(\kappa)}(\mathbf{r}_i, \mathbf{w}_j, \mathbf{w}_i)$$

over the trust region

$$2\Re\{(w_j^{(\kappa)})^H \mathbf{w}_j\} - ||w_j^{(\kappa)}||^2 > 0 \tag{8}$$

for

$$\begin{aligned}
&\lambda_{ij}^{(\kappa)}(\mathbf{r}_i, \mathbf{w}_j, \mathbf{w}_i) \triangleq \ln(1 + x_{ij}^{(\kappa)}) + y_{ij}^{(\kappa)} \\
&\times \left(2 - \frac{r_i^{(\kappa)}\bar{h}_{je}||w_j^{(\kappa)}||^2}{\mathbf{r}_i \bar{h}_{je}(2\Re\{(w_j^{(\kappa)})^H \mathbf{w}_j\} - ||w_j^{(\kappa)}||^2)} - \frac{\bar{h}_{ie}||\mathbf{w}_i||^2}{\bar{h}_{ie}||w_i^{(\kappa)}||^2}\right) \\
&= \ln(1 + x_{ij}^{(\kappa)}) + y_{ij}^{(\kappa)}\left(2 - \frac{r_i^{(\kappa)}||w_j^{(\kappa)}||^2}{\mathbf{r}_i(2\Re\{(w_j^{(\kappa)})^H \mathbf{w}_j\} - ||w_j^{(\kappa)}||^2)}\right. \\
&\quad \left. - \frac{||\mathbf{w}_i||^2}{||w_i^{(\kappa)}||^2}\right),
\end{aligned}$$

with $x_{ij}^{(\kappa)} \triangleq r_i^{(\kappa)}\bar{h}_{je}||w_j^{(\kappa)}||^2/\bar{h}_{ie}||w_i^{(\kappa)}||^2$ and $y_{ij}^{(\kappa)} \triangleq x_{ij}^{(\kappa)}/(x_{ij}^{(\kappa)} + 1)$.

Furthermore, applying inequality (72) from [14] yields $\frac{\mathbf{r}_i}{||\mathbf{w}_i||^2} \geq \beta_i^{(\kappa)}(\mathbf{r}_i, \mathbf{w}_i)$, where $\beta_i^{(\kappa)}(\mathbf{r}_i, \mathbf{w}_i) \triangleq 2(\sqrt{r_i^{(\kappa)}}/||w_i^{(\kappa)}||^2)\sqrt{\mathbf{r}_i} - (r_i^{(\kappa)}/||w_i^{(\kappa)}||^4)||\mathbf{w}_i||^2$, which is a concave function. Therefore, the nonconvex constraint (5d) is innerly approximated by the convex constraint

$$\begin{aligned}
&\bar{h}_{ie}\ln(1 - \epsilon_{\text{EV}}) + \sigma_e^2 \beta_i^{(\kappa)}(\mathbf{r}_i, \mathbf{w}_i) \\
&+ \bar{h}_{ie}\sum_{j \neq i}^{M} \lambda_{ij}^{(\kappa)}(\mathbf{r}_i, \mathbf{w}_j, \mathbf{w}_i) \geq 0, \ i \in \mathcal{M}.
\end{aligned} \tag{9}$$

Initialized from a feasible point $(w^{(0)}, R^{(0)}, r^{(0)})$ for (5), we solve the following convex optimization problem at the κth iteration to generate the next feasible point $(w^{(\kappa+1)}, R_l^{(\kappa+1)}, r_u^{(\kappa+1)})$

$$\max_{\boldsymbol{w}, \mathbf{R}, \mathbf{r}} \Phi^{(\kappa)}(\mathbf{R}, \mathbf{r}) \quad \text{s.t} \quad (3\text{b}), (5\text{b}), (8), (9), (7). \tag{10}$$

As (10) involves $n = 2M + MN_t$ variables and $m = 6M$ constraints, its computational complexity is $\mathcal{O}(n^2 m^{2.5} + m^{3.5})$. At the same κth iteration, $R_i^{(\kappa+1)}$ is then found from solving

$$\zeta_i(\mathbf{R}_i) = 0, i \in \mathcal{M} \tag{11}$$

for the increasing function $\zeta_i(\mathbf{R}_i) \triangleq f_{i,o}(\mathbf{R}_i, w^{(\kappa+1)})$ by bisection on $[R_{l,i}^{(\kappa+1)}, \eta_R R_{l,i}^{(\kappa+1)}]$ with the smallest integer η_R making $\zeta_i(\eta_R R_{u,i}) > 0$ such that[2] $-\epsilon_b \leq \zeta_i(R_i^{(\kappa+1)}) \leq 0$. Similarly, $r_i^{(\kappa+1)}$ is found from solving the nonlinear equation

$$\psi_i(\mathbf{r}_i) \triangleq g_{i,o}(\mathbf{r}_i, w^{(\kappa+1)}) = 0, i \in \mathcal{M} \tag{12}$$

by bisection on $[r_{u,i}^{(\kappa+1)}/\eta_r, r_{u,i}^{(\kappa+1)}]$ with the smallest integer η_r resulting in $\psi_i(r_{u,i}^{(\kappa+1)}/\eta_r) < 0$ such that $0 \leq \psi_i(r_i^{(\kappa+1)}) \leq \epsilon_b$.

[2] ϵ_b is the computational tolerance in solving nonlinear equations (11) and (12).

Algorithm 1: Path-following algorithm for maximin secrecy rate optimization.

Initialization: Set $\kappa = 0$. Choose an initial feasible point $(w^{(0)}, R^{(0)}, r^{(0)})$ for (5) and calculate $R_{\min}^{(0)}$ as the value of the objective function in (5) at $(w^{(0)}, R^{(0)}, r^{(0)})$.

repeat

- Solve the convex optimization problem (10) to obtain the solution $(w^{(\kappa+1)}, R_l^{(\kappa+1)}, r_u^{(\kappa+1)})$.
- Solve the nonlinear equation (12) to obtain the roots $r_i^{(\kappa+1)}$.
- Solve the nonlinear equation (11) to obtain the roots $R_i^{(\kappa+1)}$.
- Calculate $R_{\min}^{(\kappa+1)}$ as the value of the objective function in (5) at $(p^{(\kappa+1)}, R^{(\kappa+1)}, r^{(\kappa+1)})$.
- Set $\kappa = \kappa + 1$.

until $\frac{R_{\min}^{(\kappa+1)} - R_{\min}^{(\kappa)})}{R_{\min}^{(\kappa)}} \leq \epsilon_{\text{tol}}$.

Note that $(w^{(\kappa)}, R^{(\kappa)}, r^{(\kappa)})$ is a feasible point for (10) with

$$\Phi^{(\kappa)}(R^{(\kappa)}, r^{(\kappa)}) = \Phi(R^{(\kappa)}, r^{(\kappa)})$$

while $(w^{(\kappa+1)}, R^{(\kappa+1)}, r^{(\kappa+1)})$ is the optimal solution of (10), so

$$\Phi^{(\kappa)}(R^{(\kappa+1)}, r^{(\kappa+1)}) > \Phi^{(\kappa)}(R^{(\kappa)}, r^{(\kappa)})$$

as far as $(w^{(\kappa+1)}, R^{(\kappa+1)}, r^{(\kappa+1)}) \neq (w^{(\kappa)}, R^{(\kappa)}, r^{(\kappa)})$. These together with (6) yield that $(w^{(\kappa+1)}, R^{(\kappa+1)}, r^{(\kappa+1)})$ is a better feasible point for (5) than $(w^{(\kappa)}, R^{(\kappa)}, r^{(\kappa)})$

$$\begin{aligned}
\Phi(R^{(\kappa+1)}, r^{(\kappa+1)}) &\geq \Phi^{(\kappa)}(R^{(\kappa+1)}, r^{(\kappa+1)}) \\
&> \Phi^{(\kappa)}(R^{(\kappa)}, r^{(\kappa)}) \\
&= \Phi(R^{(\kappa)}, r^{(\kappa)}).
\end{aligned}$$

As such Algorithm 1, which generates a sequence $\{(w^{(\kappa)}, R^{(\kappa)}, r^{(\kappa)})\}$ of improved points for (5), converges at least to a locally optimal solution of (5) [14].

An initial feasible point $(w^{(0)}, R^{(0)}, r^{(0)})$ can be easily found as follows: take any $w^{(0)}$ feasible for the power constraint (3b) to find $R^{(0)}$ and $r^{(0)}$ by solving $f_{i,o}(\mathbf{R}_i, w^{(0)}) = 0$ and $g_{i,o}(\mathbf{r}_i, w^{(0)}) = 0, i \in \mathcal{M}$.

IV. SEE Maximization

We return to the SEE maximization problem (4), which can be shown to be equivalent to the following problem:

$$\max_{\boldsymbol{w}, \mathbf{R}, \mathbf{r}} \Theta(\mathbf{w}, \mathbf{R}, \mathbf{r}) \quad \text{s.t.} \quad (3\text{b}), (4\text{b}), (5\text{b}), (5\text{c}), (5\text{d}). \tag{13}$$

To avoid Dinkelbach's iterations, which invoke the solution of a difficult nonconvex optimization problem (see, e.g., [10]), which is as computationally difficult as (13) itself, a more direct approach (see, e.g., [4]) is based on a lower bounding approximation for the objective function Θ. We now propose another approach to tackle (13), under which the SEE maximization problem (13) is no more computationally difficult than the secrecy rate maximization problem (5).

Let $(w^{(\kappa)}, R^{(\kappa)}, r^{(\kappa)})$ be a feasible point for (13) found from the $(\kappa-1)$th iteration. At the κth iteration, we solve the following convex optimization problem to generate $(w^{(\kappa+1)}, R_l^{(\kappa+1)}, r_u^{(\kappa+1)})$:

$$\max_{\boldsymbol{w},\mathbf{r}} \Psi^{(\kappa)}(\mathbf{w},\mathbf{R},\mathbf{r}) \quad \text{s.t.} \quad (3b), (8), (9), (5b), (7),$$

$$A_i^{(\kappa)}(\mathbf{R}_i) - a_i^{(\kappa)}(\mathbf{r}_i) \geq c_i, i \in \mathcal{M} \tag{14}$$

where $\Psi^{(\kappa)}(\mathbf{w},\mathbf{R},\mathbf{r}) \triangleq \sum_{i=1}^M [A_i^{(\kappa)}(\mathbf{R}_i) - a_i^{(\kappa)}(\mathbf{r}_i)] - \Theta(w^{(\kappa)}, R^{(\kappa)}, r^{(\kappa)})\pi(\mathbf{w})$. Further, $r_i^{(\kappa+1)}$ is found from solving (12), while $R_i^{(\kappa+1)}$ is found from solving (11).

Note that $(w^{(\kappa)}, R^{(\kappa)}, r^{(\kappa)})$ is a feasible point for (13) with $\Psi^{(\kappa)}(w^{(\kappa)}, R^{(\kappa)}, r^{(\kappa)}) = 0$, while $(w^{(\kappa+1)}, R^{(\kappa+1)}, r^{(\kappa+1)})$ is the optimal solution of (14), so

$$\Psi^{(\kappa)}(w^{(\kappa+1)}, R^{(\kappa+1)}, r^{(\kappa+1)}) > 0$$

as far as $(w^{(\kappa+1)}, R^{(\kappa+1)}, r^{(\kappa+1)}) \neq (w^{(\kappa)}, R^{(\kappa)}, r^{(\kappa)})$, which means $\sum_{i=1}^M [A_i^{(\kappa)}(R_i^{(\kappa+1)}) - a_i^{(\kappa)}(r_i^{(\kappa+1)})]/\pi(w^{(\kappa+1)}) > \Theta(w^{(\kappa)}, R^{(\kappa)}, r^{(\kappa)})$. Therefore, $\Theta(w^{(\kappa+1)}, R^{(\kappa+1)}, r^{(\kappa+1)}) = \sum_{i=1}^M \frac{\ln(1+R_i^{(\kappa+1)}) - \ln(1+r_i^{(\kappa+1)})}{\pi(w^{(\kappa+1)})} \geq \sum_{i=1}^M \frac{A_i^{(\kappa)}(R_i^{(\kappa+1)}) - a_i^{(\kappa)}(r_i^{(\kappa+1)})}{\pi(w^{(\kappa+1)})} > \Theta(w^{(\kappa)}, R^{(\kappa)}, r^{(\kappa)})$, i.e., $(w^{(\kappa+1)}, R^{(\kappa+1)}, r^{(\kappa+1)})$ is a better feasible point for (13) than $(w^{(\kappa)}, R^{(\kappa)}, r^{(\kappa)})$. Thus, similar to Algorithm 1, a path-following algorithm for (13), which solves the convex optimization problem (14) to iterate feasible points, will converge at least to a locally optimal solution.

V. Numerical Examples

This section presents numerical results to demonstrate the efficiency of the proposed algorithms. Each transmitter is equipped with $N_t = 4$ antennas. The scenario of $M = 5$ pairs with the noise variance $\sigma_i^2 = \sigma_e^2 = 1$ mW is simulated. The drain efficiency $1/\zeta$ of the power amplifier is 40% with the circuit power of each transmit antenna $P_a = 1.25$ mW. The computation tolerance for terminating all proposed algorithms is $\epsilon_{\text{tol}} = 10^{-4}$. We divide the obtained secrecy rate results by $\ln(2)$ to arrive at the unit of bps/Hz (in secrecy rate) and bits/J/Hz (in SEE).

Like [7] and [8], we choose $\bar{h}_{ii} = 1$, and generate $\bar{h}_{ji} \in \lambda C(0,1)$ with $0 < \lambda < 1$, which expresses the channel interference degree. We generate $\bar{h}_{je} \in \lambda_{\text{EV}} C(0,1)$ with $\lambda_{\text{EV}} = 0.5$ for EV in a bad position, $\lambda_{\text{EV}} = 1$ for EV in a medium position, and $\lambda_{\text{EV}} = 1.5$ for EV in a very good position.

The performance of CDI-based secure beamforming for secrecy rate maximin optimization via (3) is analyzed first. Fig. 1 plots the users' minimum secrecy rate versus the transmit power limitation P_i varying from 5 to 25 mW. The minimum secrecy rate increases with the transmit power limitation P_i. This secrecy rate for the interfering degree $\lambda = 0.2$ is better than that achieved for the interfering degree $\lambda = 0.7$. This figure also shows that those rates for the strong eavesdropping degree $\lambda_{\text{EV}} = 1.5$ are worse than their counterparts for weaker eavesdropping degrees $\lambda_{\text{EV}} = 0.5$ and $\lambda_{\text{EV}} = 1$.

Next, the SEE performance of beamforming via (4) is analyzed. The threshold c_i for the QoS constraint (4b) is 0.035 bps/Hz and the transmit power limitation P_i still varies from 5 to 25 mW. It is clear from Fig. 2 that the SEE performance saturates when the transmit power budget exceeds a threshold.

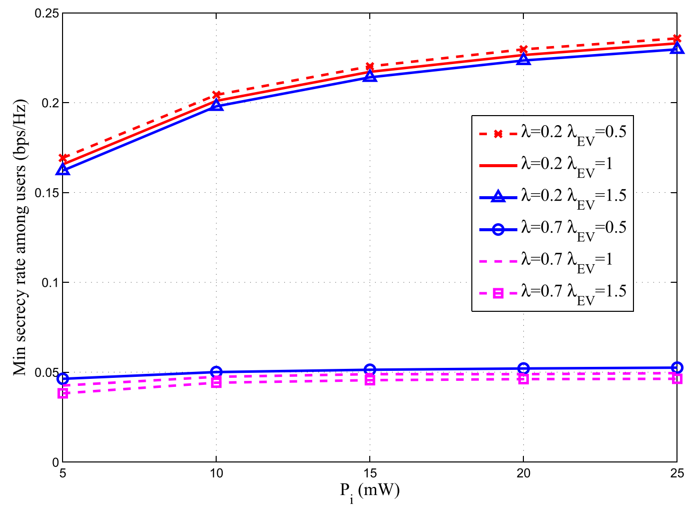

Fig. 1. Minimum secrecy rate among users versus the transmit power limitation P_i with $M = 5$.

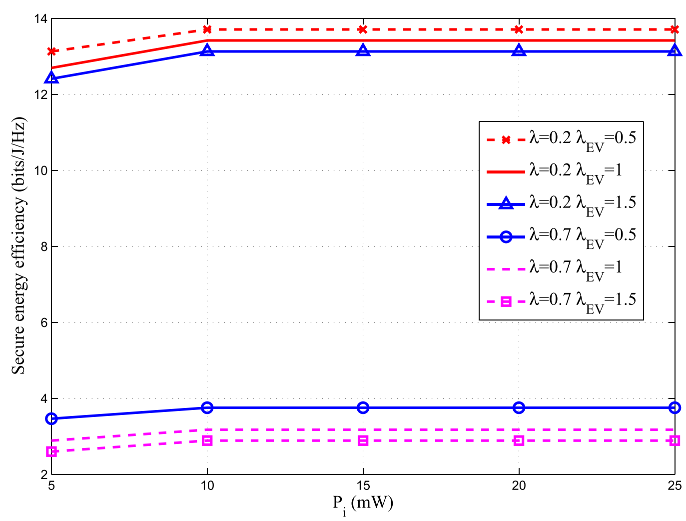

Fig. 2. Energy efficiency versus the transmit power limitation P_i with $M = 5$.

This is due to the fact that for small transmit power ranges, the denominator of SEE is dominated by the circuit power and thus SEE is maximized by maximizing the secrecy rate sum in the numerator. However, for large transmit power ranges, the denominator of SEE is actually dominated by the actual transmit power in the denominator.

VI. Conclusion

Based on the knowledge of the channel distributions of a multi-input single-output (MISO) wireless interference network overheard by an eavesdropper, we have proposed path-following algorithms for the beamformer design to maximize either its users' secrecy rate or its SEE. Numerical results have been provided to clarify the algorithms' efficiency as well as the role of beamforming in protecting secure multiuser communication. Extensions to secure beamforming in multi-input multi-output interference networks with multiantenna eavesdroppers are under current investigation.

REFERENCES

[1] A. Mukherjee and A. L. Swindlehurst, “Robust beamforming for security in MIMO wiretap channels with imperfect CSI,” *IEEE Trans. Signal Process.*, vol. 59, no. 1, pp. 351–361, Jan. 2011.

[2] J. Park, Y. Sung, D. Kim, and H. V. Poor, “Outage probability and outage-based robust beamforming for MIMO interference channels with imperfect channel state information,” *IEEE Trans. Wireless Commun.*, vol. 11, no. 10, pp. 3561–3573, Oct. 2012.

[3] A. A. Nasir, H. D. Tuan, T. Q. Duong, and H. V. Poor, “Secrecy rate beamforming for multicell networks with information and energy harvesting,” *IEEE Trans. Signal Process.*, vol. 65, no. 3, pp. 677–689, Feb. 2017.

[4] A. A. Nasir, H. D. Tuan, T. Q. Duong, and H. V. Poor, “Secure and energy-efficient beamforming for simultaneous information and energy transfer,” *IEEE Trans. Wireless Commun.*, vol. 16, no. 11, pp. 7523–7537, Nov. 2017.

[5] L. Liu, R. Zhang, and K.-C. Chua, “Secrecy wireless information and power transfer with MISO beamforming,” *IEEE Trans. Signal Process.*, vol. 62, no. 7, pp. 1850–1863, Apr. 2014.

[6] N. Nguyen, H. D. Tuan, T. Q. Duong, and H. V. Poor, “MIMO beamforming for secure and energy-efficient wireless communication,” *IEEE Signal Process. Lett.*, vol. 24, no. 2, pp. 236–239, Feb. 2017.

[7] W. Li, T. Chang, C. Lin, and C. Chi, “Coordinated beamforming for multiuser MISO interference channel under rate outage constraints,” *IEEE Trans. Signal Process.*, vol. 61, no. 5, pp. 1087–1102, Mar. 2013.

[8] W. Li, T. Chang, and C. Chi, “Multi-cell coordinated beamforming with rate outage constraint-part II: Efficient approximation algorithms,” *IEEE Trans. Signal Process.*, vol. 63, no. 11, pp. 2763–2778, Jun. 2015.

[9] D. Wang, B. Bai, W. Chen, and Z. Han, “Achieving high energy efficiency and physical-layer security in AF relaying,” *IEEE Trans. Wireless Commun.*, vol. 15, no. 1, pp. 740–752, Jan. 2016.

[10] S. Buzzi, C.-L. I, T. E. Klein, H. V. Poor, C. Yang, and A. Zappone, “A survey of energy-efficient techniques for 5G networks and challenges ahead,” *IEEE J. Sel. Areas Commun.*, vol. 34, no. 4, pp. 697–709, Apr. 2016.

[11] V. S. Annapureddy and V. V. Veeravalli, “Sum capacity of MIMO interference channels in the low interference regime,” *IEEE Trans. Inf. Theory*, vol. 57, no. 5, pp. 2565–2581, May 2011.

[12] E. Che, H. D. Tuan, H. H. M. Tam, and H. H. Nguyen, “Successive interference mitigation in multiuser MIMO channels,” *IEEE Trans. Commun.*, vol. 63, no. 6, pp. 2185–2199, Jun. 2015.

[13] Z. Sheng, H. D. Tuan, A. A. Nasir, T. Q. Duong, and H. V. Poor, “Power allocation for energy efficiency and secrecy of wireless interference networks,” *IEEE Trans. Wireless Commun.*, to be published.

[14] Z. Sheng, H. D. Tuan, T. Q. Duong, and H. V. Poor, “Beamforming optimization for physical layer security in MISO wireless networks,” *IEEE Trans. Signal Process.*, 2018 (Early Access).